Electronic Supplementary Material (ESI) for Soft Matter.

Supporting Information

Measurement of long range attractive forces between hydrophobic surfaces produced by vapor phase adsorption of palmitic acid

Namsoon Eom †, DrewF. Parsons ‡ and Vincent S. J. Craig † *

† Department of Applied Mathematics, Research School of Physics and Engineering, Australian National University, Canberra, ACT, 2601, Australia

‡ School of Engineering and IT, Murdoch University, 90 South Street, Murdoch, Western Australia 6150, Australia

Sections

1. *Film thickness from ellipsometry*
2. *Reproducibility across different locations*
3. *The attraction is exponential*
4. *Interaction Area between approaching surfaces*
5. *AFM Images of the PA-Hafnia surface*
6. *Mutlilayered van der Waals interactions*
7. *Interaction forces measured in 0.01 M NaCl*

1. Film thickness from ellipsometry

The thickness of the palmitic acid layer formed on the hafnia surface after vapor treatment at 135 °C for 60 min was determined using an ellipsometry (M2000D, JA Woollam) as shown in Figure S1. The thickness and the refractive index of the palmitic acid layer estimated using a Cauchy model were 1.0 ± 0.3 nm and 1.5 ± 0.1 (at 630 nm), respectively.

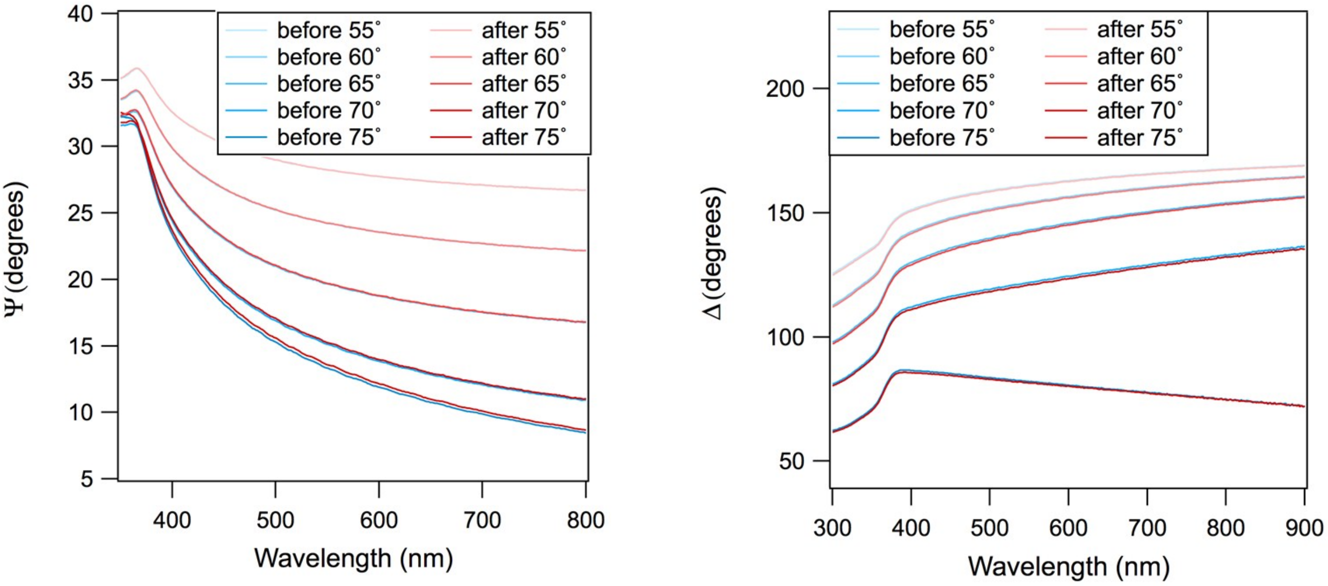

Figure S1. Measured spectra (Ψ, Δ) of ALD hafnia surface before and after treatment with palmitic acid.

2. Reproducibility across different locations

The forces measured at three different locations for each pH are consistent as shown in Figure S2. Little variation was observed between different locations, implying that surface nanobubbles are not responsible for the attraction observed in the measured forces.

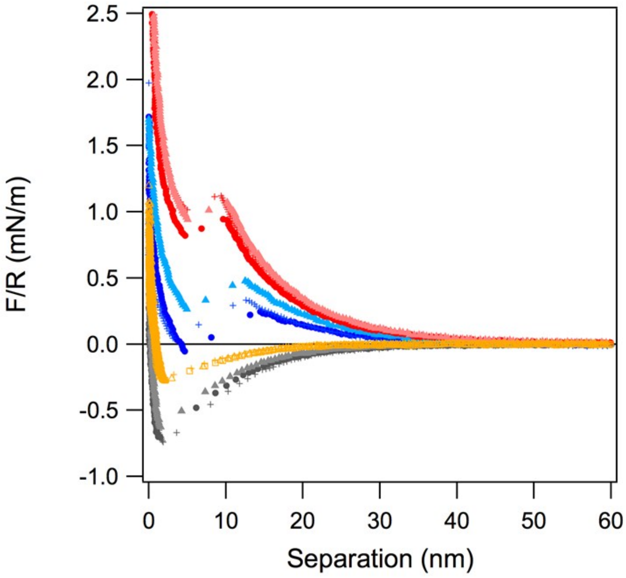

Figure S2. Normalised force versus separation measured between PA hafnia surfaces prepared at 135 °C for 60 min, in three different locations at pH 3.2 (Grey), pH 2.6 (Orange), pH 5.2 (Blue), and pH 7.2 (Red).

3. *The attraction is exponential*

The measured normalized force versus separation measured at pH 2.6 and pH 3.2 were fitted with the Van der Waals interaction and an additional exponential attraction. The fit is shown in Figure S3. The decay length waas found to be 6.0 nm at pH 2.6 and 7.1 nm at pH 3.2. This is comparable to the Debye lengths for these solutions of 5.1 nm and 7.5 nm respectively.

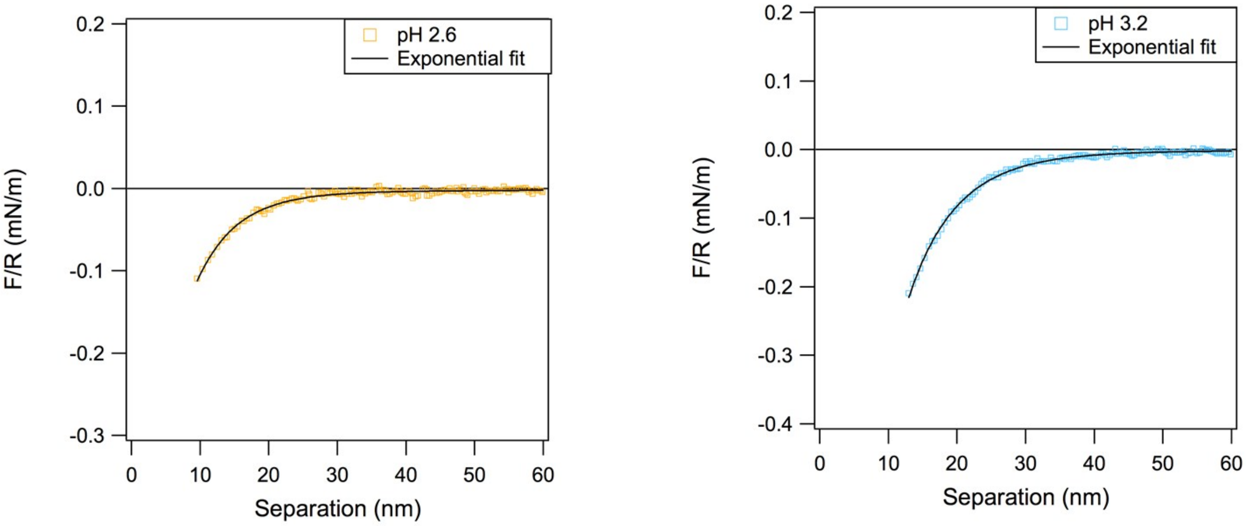

Figure S3: Exponential fit to the attractive force curves obtained at pH 2.6 and pH 3.2 in 0.001M NaCl. Here, the van der Waals component is subtracted from the data for the exponential fit. The decay length is 6.0 nm with a pre-factor of 0.52 mN/m at pH 2.6 and 7.1 nm with a pre-factor of 1.3 mN/m at pH 3.2.

4. *Interaction Area between approaching surfaces*

We apply the Langbein approximation to determine the effective area of interaction between the spherical colloid probe and the flat substrate. This requires knowledge of the radius of the sphere and the range of the interaction.

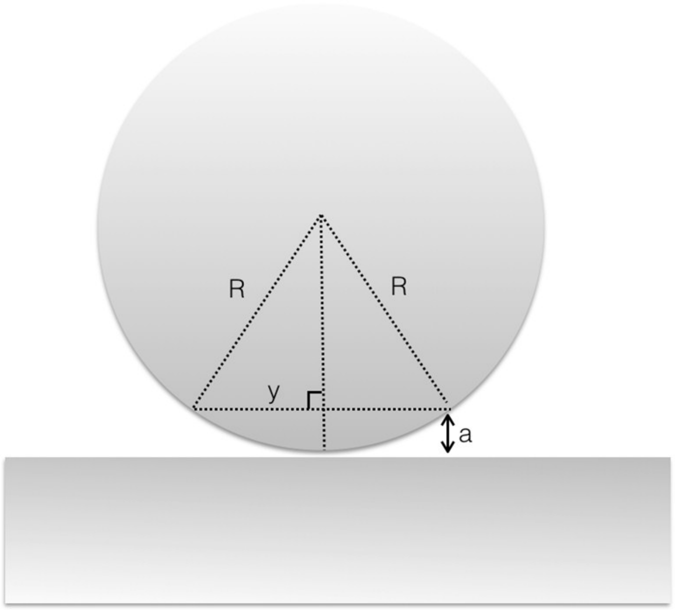

Figure S4: A schematic of the effective interaction area of a colloid probe with radius R when it interacts over a distance, a, with a flat surface

The effective area of interaction depends on the range of the force, a. The area of interaction of a colloid probe with radius R (Figure S5) then is πy^2. By the Pythagoras theorem,

$$R^2 = y^2 + (R - a)^2,$$

And thus,

$y^2 = 2Ra - (a)^2$

The area of interaction then depends on the radius R and the range of the force a,

$\pi y^2 = \pi\left(2Ra - (a)^2\right) = \pi a(2R - a)$

For a colloid probe with radius R = 10 μm, and and interaction force that extends to a distance of a = 30 nm, the area of interaction is 1.9 $\times 10^6\ nm^2$, or a circle with radius 778 nm. Therefore if the bilayer patches are separated by more than this distance, it is likely that a single patch on one surface will interact with a single patch on the other surface.

5. *AFM Images of the PA-Hafnia surface*

In order to determine if patches form spontaneously when the PA-hafnia surface is immersed in aqueous solution a PA-hafnia surface was imaged using an AFM both in air and in solution and again in air (see Figure 10 o the manuscript). Images were obtained using a Bruker Multimode VIII AFM in ScanAsyst mode with ScanAsyst Air and ScanAsyst fluid cantilevers as appropriate. Images in solution were obtained using a closed fluid cell. The images obtained were homogenous and smooth consistent with a single monolayer of PA on the surface both in air and in water. In one location evidence of bilayered patches of PA were observed and these are shown in figure S5. During injection of water onto the surface bubbles are initially trapped on the surface. It is possible that the bilayered structures observed in figure S5 may be formed during this process. Elsewhere the surfaces were very uniform and there was no evidence of such bilayers. We note that the force measurements were found to be reproducible from one location to the next supporting the observation that the surfaces are initially homogenous and that bilayered patches are formed during approach of the surfaces.

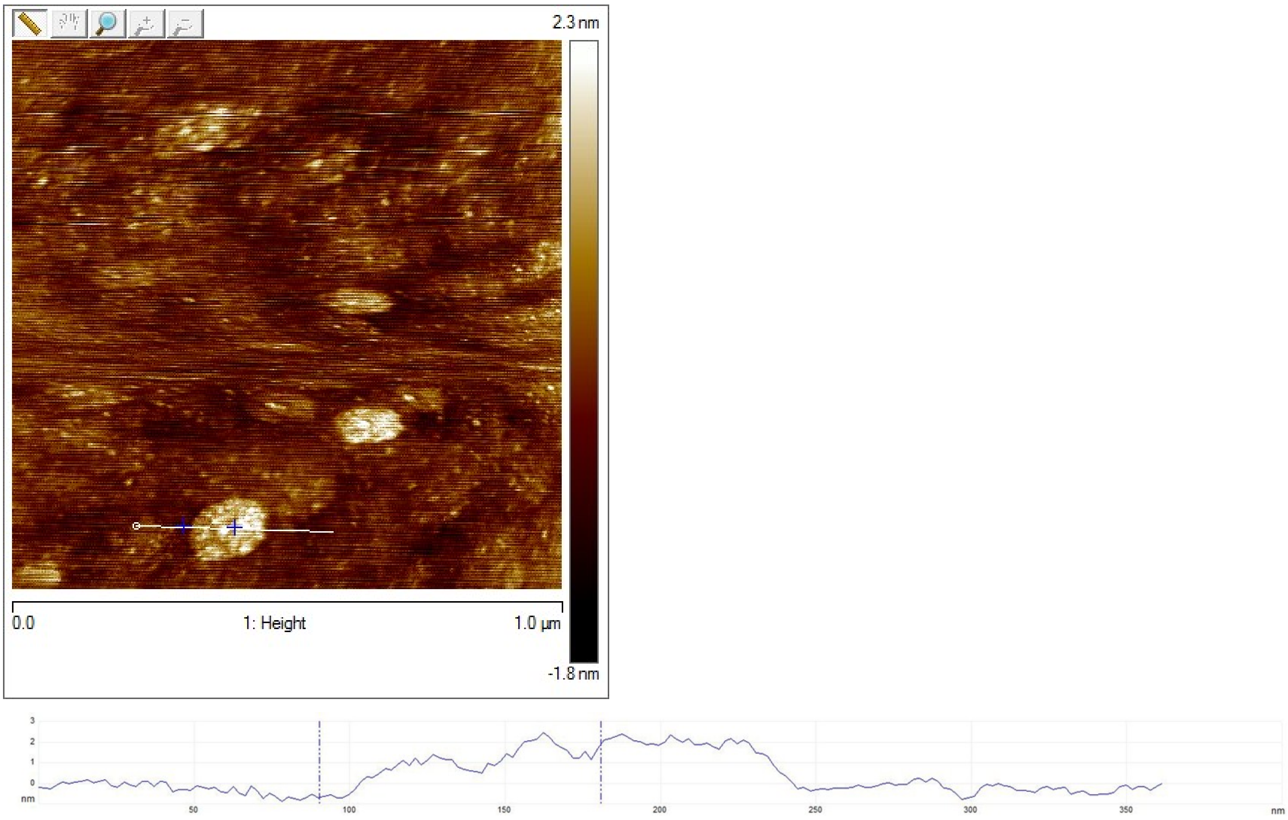

Figure S5: AFM height image of the same PA-hafnia surface as above imaged in water with a section across a feature as shown by the white line in the image. 1 µm x 1 µm scan. Note the image is blurred in places as the O-ring acts to couple the motion of the surface to the cantilever, reducing the quality of the image. The height of the section (~ 2m above the background) suggests that the lighter features are bilayered patches of palmitic acid adjacent to patches of bare surface. Note this was only observed at this location and all other locations investigated did not show such features.

6. *Mutlilayered van der Waals interactions*

The palmitic acid coated hafnia surface is a multilayer surface constructed from a silicon substrate covered in SiO_2 (nm), TiO_2 (nm), HfO_2 (nm) with a 1 nm outer coating of palmitic acid, see Figure S6.

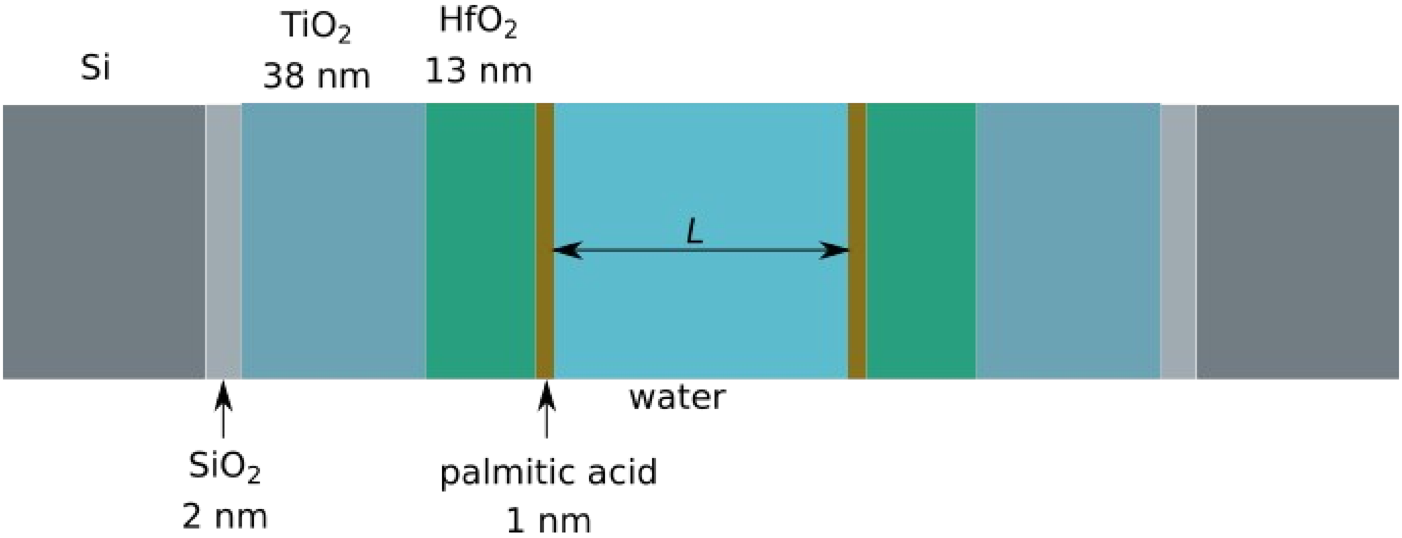

Figure S6: Schematic of the multilayer palmitic acid coated hafnia surface.

It is convenient to model the forces measured by AFM (sphere-plane geometry) using the proximity force approximation (Derjaguin approximation) based on the interaction free energy $F_{vdW}(L)$ between two planes. The van der Waals interaction energy between two such planar multilayer surfaces may be described via a distance-dependent Hamaker coefficient $A(L)$,

$$F_{vdW}(L) = \frac{-A(L)}{12\pi L^2} \tag{S1}$$

The Hamaker coefficient is evaluated in the usual way via a dielectric function $\varepsilon_s(i\omega)$ for each surface[1, 2] ,

$$A(L) = \frac{2kT}{3}\sum\int dxx\{ln[1-\grave{\Delta}_{mL}(i\omega_n)\grave{\Delta}_{mR}(i\omega_n)e^{-x}] + ln[1-\Delta_{mL}(i\omega_n)\Delta_{mR}(i\omega_n)e^{-x}]\} \tag{S2}$$

where ω_n are the Matsubara frequencies $\omega_n = 2\pi kTn/\hbar$. The prime next to the summation symbol indicates that *n*=0 is taken with a factor ½.$r_n = 2L\omega_n\sqrt{\varepsilon_m(i\omega_n)}$$\grave{\Delta}$and $\Delta$are dielectric and diamagnetic reflection coefficients,.

$$\grave{\Delta}_{jk}(i\omega) = \frac{s_j\varepsilon_j - s_j\varepsilon_k}{s_j\varepsilon_j + s_j\varepsilon_k}$$

S3

and

$$\Delta_{jk}(i\omega) = \frac{s_j\mu_j - s_j\mu_k}{s_j\mu_j + s_j\mu_k}$$

S4

We take the materials to be nonmagnetic such that μ_i=1 for each layer. s_i is a retardation coefficient, $s_j(i\omega) = \sqrt{p^2 - 1 + \varepsilon_j(i\omega)/\varepsilon_m(i\omega)}$where $p = xc/2\omega L\sqrt{(\varepsilon_m(i\omega))}$. The dielectric functions ε_i in Eq. S3 may be thought of as an effective dielectric function describing the combined response of all layers. But more precisely it refers to the dielectric function of each layer in turn, in which case the reflection coefficients in Eq. S2 are determined recursively from neighbouring layers,

$$\Delta_{mL} = \frac{\Delta_{m,1} + \Delta_{1,L}e^{-xs_1l_1/pL}}{1 + \Delta_{m,1}\Delta_{1,L}e^{-xs_1l_1/pL}}$$

S5

and

$$\Delta_{jL} = \frac{\Delta_{j,j+1} + \Delta_{j+1,L}e^{-xs_{j+1}l_{j+1}/pL}}{1 + \Delta_{j,j+1}\Delta_{j+1,L}e^{-xs_{j+1}l_{j+1}/pL}}$$

Because of the appearance of separation distance *L* in these recursive reflection coefficients, the Hamaker coefficient becomes distance-dependent even in the nonretard limit *c*→∞.

The distance-dependant Hamaker coefficient (retarded and nonretarded) for our palmitic acid coated hafnia surface is shown in Figure S7 (the dielectric function of palmitic acid is presented using that of hexadecane). Nonretarded Hamaker constants for each layer (pure solid – water – pure solid) are also shown for comparison. At short range below 10 nm the Hamaker coefficient is small, due to the outer palmitic acid layer. It rises to the value of hafnia at mid-range 10-100 nm. At large separations greater than 200 nm the Hamaker coefficient is controlled by the underlying silicon substrate, and is attenuated by retardation such that the value of the retarded Hamaker coefficient never exceeds that of pure hafnia.

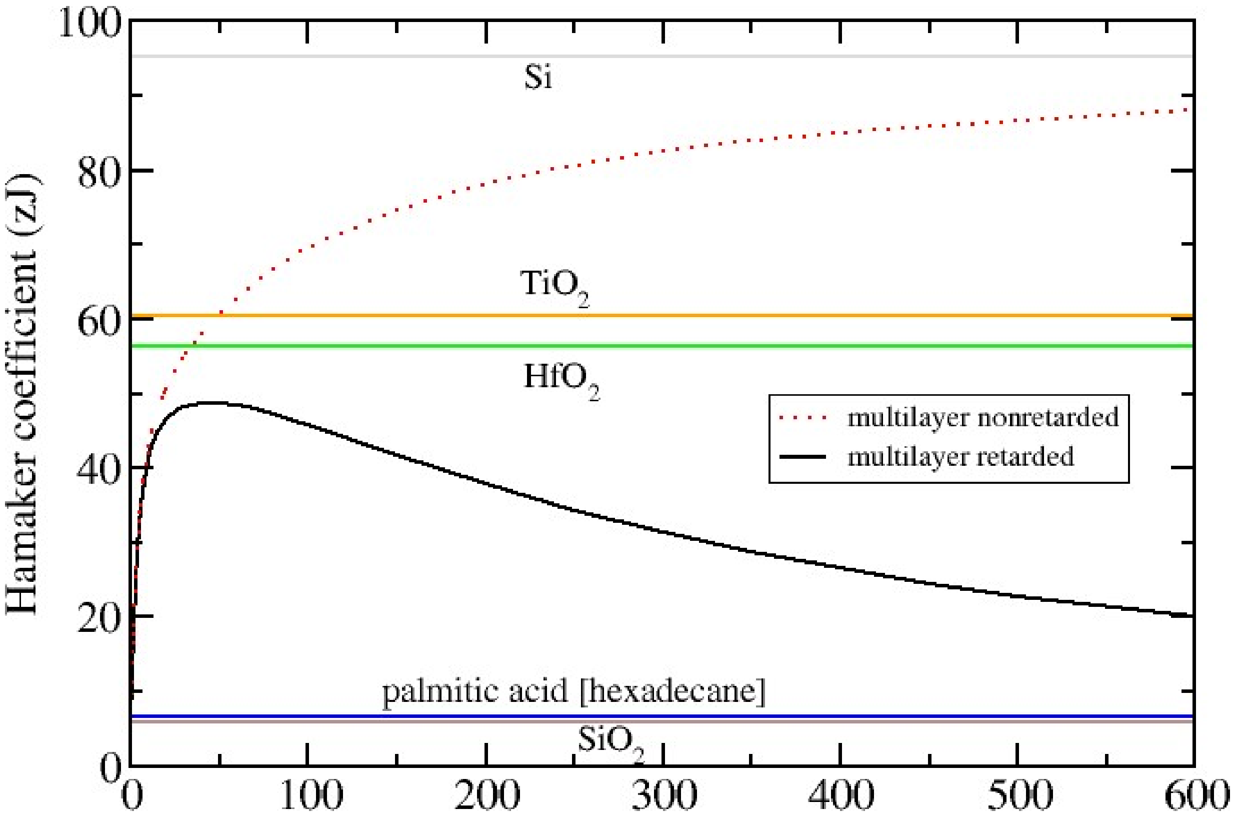

Figure S7: Distance-dependent Hamaker coefficient for the multilayered palmitic acid coated hafnia surface. Both retarded and nonretarded Hamaker coefficients are shown, as well as the nonretarded Hamakers constants (solid-water-solid) of each layer.

7. Interaction forces measured in 0.01 M NaCl

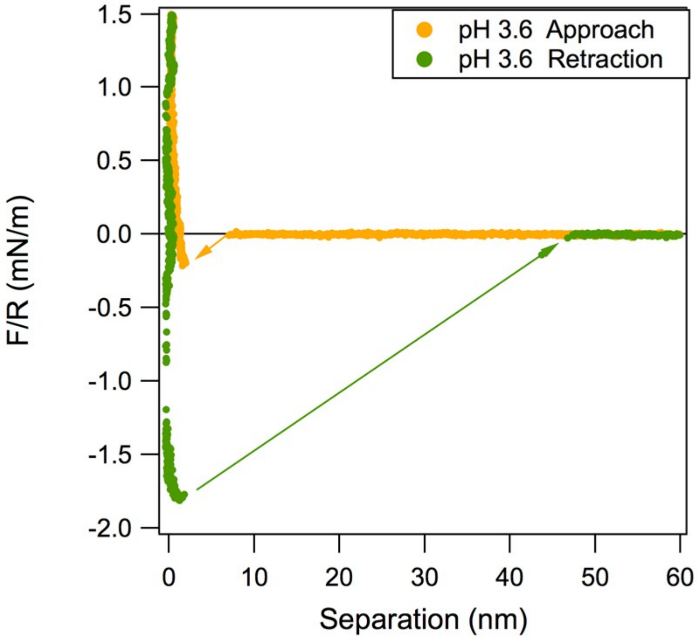

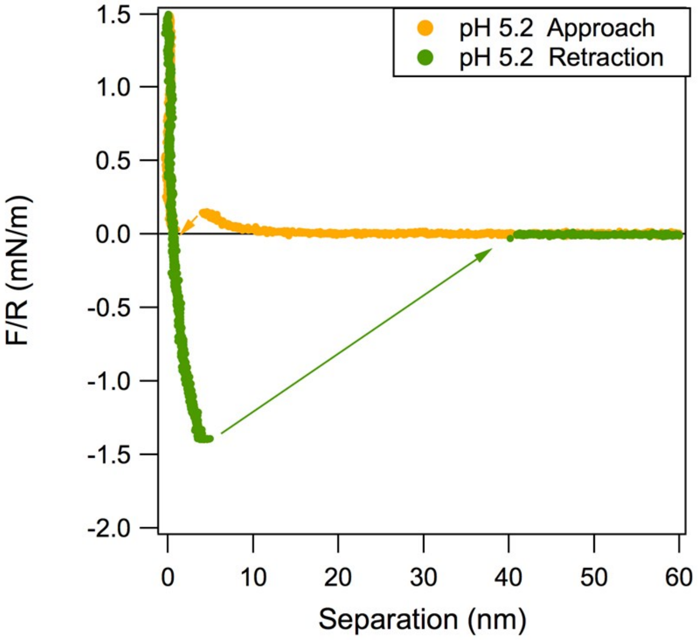

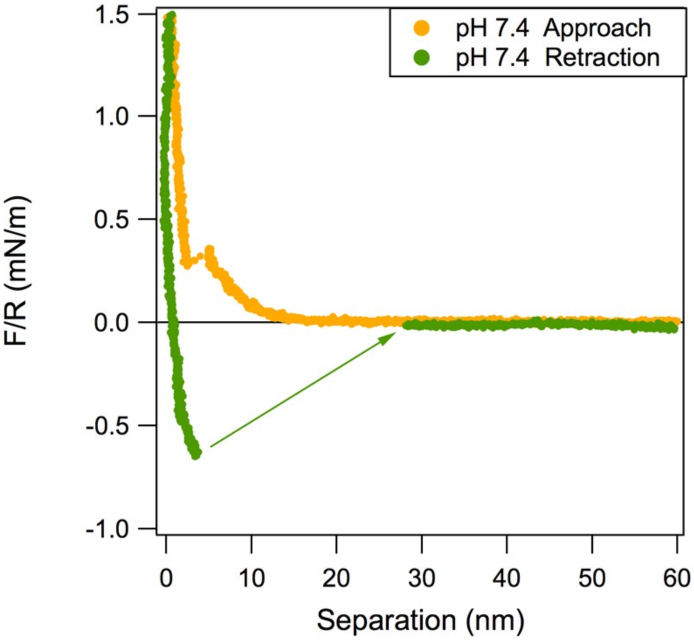

Figure S8: The normalized force (F/R) measured as a function of separation between PA-hafnia surfaces prepared at 135 °C for 60 min at pH 3.6 (top), pH 5.2 (middle), and pH 7.4 (bottom) during approach and retraction in 0.01 M NaCl solution. A cantilever with spring constant of 0.39 N/m was used. Force measurement were performed at scan rate of 1 Hz with ramp size of 500 nm.

References

1. V. A. Parsegian and B. W. Ninham, *Journal of theoretical biology*, 1973, **38**, 101-109.
2. R. Walsh, A. Nelson, W. M. Skinner, D. Parsons and V. S. J. Craig, *Journal of Physical Chemistry C*, 2012, **116**, 7838-7847.